EXPERIMENTAL AND NUMERICAL APPROACHES OF AEROSOLS REMOVAL IN SPRAY FOR NUCLEAR REACTOR CONTAINMENT APPLICATION

E. Porcheron, P. Lemaitre, D. Marchand, A. Nuboer, and J. Vendel

Institut de Radioprotection et de Sûreté Nucléaire (IRSN)
BP 68, 91192 Gif-sur-Yvette cedex, France
emmanuel.porcheron@irsn.fr

ABSTRACT

TOSQAN is an experimental program undertaken by the Institut de Radioprotection et de Sûreté Nucléaire (IRSN) in order to perform thermal hydraulic containment studies. The TOSQAN facility is a large enclosure devoted to simulate typical accidental thermal hydraulic flow conditions in nuclear Pressurized Water Reactor (PWR) containment. The TOSQAN facility, which is highly instrumented with non-intrusive optical diagnostics, is particularly adapted to nuclear safety CFD code validation. The present work is devoted to study the interaction of a water spray injection used as a mitigation means in order to reduce the gas pressure and temperature in the containment, to produce gases mixing and washout of fission products. In order to have a better understanding of heat and mass transfers between the spray droplets and the gas mixture, and to analyze mixing effects due to spray activation, we performed detailed characterization of the two-phase flow.

Key words: Thermal hydraulic, TOSQAN, Containment, Spray, Heat and mass transfers, Aerosol, Fission products

1 INTRODUCTION

During the course of a hypothetical severe accident in a Pressurized Water Reactor (PWR), hydrogen may be produced by the reactor core oxidation and can be distributed into the reactor containment by convection flows and steam condensation on walls. In order to assess the risk of detonation generated by a high local hydrogen concentration, the hydrogen distribution in the containment has to be known. In addition, core degradation leads to fission products release into the containment. The most important part of the fission products is emitted in the particulate form (size close to 1 µm[1]). They are mixed with aerosol resulting from degradation of structural materials such as control rods, ducts, for which granulometry is lower than 100 µm, with a material average density of 3 g.cm^{-3}. Only a fraction of the formed aerosol with a granulometry ranging below 5 µm may migrate from the primary circuit towards the containment. Water spraying in the containment is used as a mitigation means in order to reduce pressure, to remove fission products and to enhance the gas mixing in case of the presence of hydrogen.

The TOSQAN experimental program has been created to simulate typical thermal hydraulic conditions representative of a severe accident in the reactor containment. The specificity of the TOSQAN facility is characterized by a high level of instrumentation that provides detailed information on local and non-intrusive characterization of the two-phase flow for CFD code validation[2].

The present work is dedicated to study the effect of a water spray activation used as a mitigation means in order to reduce steam containment pressure, to decrease the local hydrogen concentration by the mixing caused by spray entrainment and steam condensation on droplets, and to washout aerosol to the sump. In order to have a better understanding of physical phenomena, a detailed characterization of the spray and the gas is needed. Spray tests are performed in hot conditions to analyze the heat and mass transfers between spray droplets and gas mixtures composed of air and steam, or dry air, and the aerosol washout.

In this paper, we present the analysis of water spray interaction with gaseous mixtures composed of air and steam, seeded with aerosol, in order to study, on the first hand, the heat and mass transfers between droplets and gas and, on the other hand, the aerosol removal processes by spray. This work is divided into three parts. The first part is devoted to present the TOSQAN facility, the instrumentation used and its principles. In the second part, an analysis of spray interaction with the air and steam mixture is performed. In the third part, we focus on the aerosol washout and we determine the aerosol collection efficiency for single droplet and for the global spray.

2 EXPERIMENTAL FACILITY AND TEST PROCEDURE

2.1. The TOSQAN vessel

The TOSQAN facility shown in Fig.1 consists of a closed cylindrical vessel (7 m^3 volume, 4 m high, 1.5 m internal diameter) into which steam is injected.
The walls of the vessel are thermostatically controlled by heated oil circulation to control the gas temperature inside the vessel. Optical accesses are provided by 14

pressure resistant viewing windows permitting non-intrusive optical measurements along orthogonal enclosure diameters.
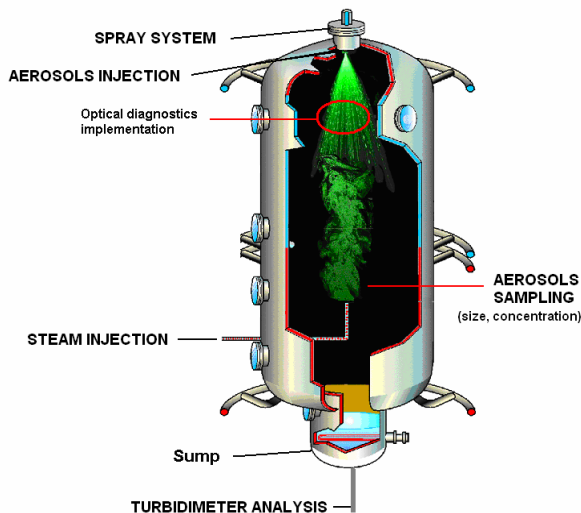

Fig.1 Overview of the TOSQAN facility.

The inner spray system, located in the dome of the enclosure on the vertical axis, is composed of a single nozzle producing a full cone water spray. This nozzle is mobile along the vertical axis so that measurements can be made at different distances from the nozzle in order to be able to precisely mesh the close field of the spray injection. Aerosols, which are used for fission products simulation, are injected into the top of the dome of the vessel by the means of a powder spreader.

2.2 Instrumentation

Both intrusive and non-intrusive techniques are implemented on the TOSQAN facility in order to achieve a detailed characterization of the spray droplets, the aerosols and the gas.

2.2.1 Description of intrusive techniques

Over 100 thermocouples are used to measure the gas temperature in the whole vessel. Thermocouples are located along the vessel diameter at 6 different levels distributed along the TOSQAN height. Other thermocouples are located in the sump and dome regions, and near the heated walls. The mass spectrometry technique is used for gas concentrations measurements. The sampling system is composed of 9 heated lines, each connected via a rotating valve to 6 fine tubes which provide 54 sampling points located at different heights and radii[3]. Aerosol mass concentration ($C_{aerosol}(0)$) and size distribution ($D_{aerosol}$) in the gas phase are measured, during the test, using an optical granulometer[4]. Aerosol sampling is realized in the spray region. The water which is drained out of the vessel at the sump level is analyzed using a prototype online turbidimeter, in order to determine the aerosol mass ($M_{aerosol\_collected}$) collected by droplets during their fall (Fig.1). Because the water spray falling into the sump is removed with the same injected water mass flow, there is no water accumulation in the sump, and therefore it is empty during all along the test.

2.2.2 Description of non-intrusive techniques

Droplets velocity measurements are performed with two kinds of commercial optical diagnostics such as the Particle Image Velocimetry technique (PIV) and Laser Doppler Velocimetry technique (LDV). Both techniques are based on Mie scattering derived by the light generated by the interaction between particles (water droplets or seeding) and a laser beam. The LDV technique provides local information on the Turbulence Intensity (TI) and on two velocity components, the vertical one (V) and the radial one (U) (Table 1). The PIV technique provides instantaneous or mean velocity fields of the flow (Table 1). Various kinds of measurement techniques are available for analyzing the spray droplets size distribution, such as the Phase Doppler Anemometry (PDA). The PDA[5] technique cannot be used in the TOSQAN facility because of optical access constraints. This is why we decided to use the Interferometrics Laser Imaging for Droplet Sizing (ILIDS)[6]. For gas volume fraction measurements, we use the Spontaneous Raman Scattering spectroscopy (SRS)[7]. The accuracy of the instrumentation used on the TOSQAN facility is detailed in the quoted references and is summarized in Table 1.

Table 1. TOSQAN instrumentation accuracy

	Techniques	Physical magnitude	Accuracy
Droplets	LDV	V, U (m/s) TI	1% to 5%
	PIV	V, U (m/s)	2% to 10%
	ILIDS	$D_{droplet}$ (µm)	5%
Gas	SRS	X_{steam} , X_{air} (%)	+/- 1 Vol%
	Mass spectrometry	X_{steam} , X_{air} (%)	+/- 1.5 Vol%
	Thermocouple	T (°C)	+/- 1°C
Aerosol	Optical spectrometer	$D_{aerosol}$ (µm) $C_{aerosol}$ (mg/m³)	µm 5%
	Turbidimeter	$M_{aerosol\_collected}$ (mg)	7%

2.3 Test procedure

Test scenario consists in water spray injection in the TOSQAN vessel which is initially seeded with aerosol simulating fission products release, and after, pressurized with steam, simulating the primary circuit breach (Table 2). Aerosols are initially injected into the vessel which has a gas leak in order to stay at atmospheric pressure during the aerosols injection phase. Aerosol concentration in suspension in the vessel is measured in real time by using the WELAS granulometer that allows good reproductibility of the initial test conditions. This measurement is also used to determine the total aerosol mass present in the gas of the vessel all along the test and particularly just before the spray activation, since it is not able to measure accurately the aerosol mass injected in the vessel. The aerosol chosen for this study are particles of silicon carbide (SiC) with a granulometry ranging below 5 µm and material density of 3.2 g.cm^{-3} (see Table 3). The spray nozzle used is fed with a water mass flow rate equal to 30 g.s^{-1} and a water temperature equal to 20°C. However, at the beginning of the spray activation (t < 30 s), the temperature of the water injected is above 30°C because the water which is initially present in the spray circuit is heated by conduction from the vessel. The heated walls of the TOSQAN vessel are also fixed at the same temperature all along the spray test (120°C).

Table 2. Spray specifications

Water injection temperature	Droplets arithmetic mean diameter (D$_{droplet}$)	Gas mixture composition (bar)	
		air	steam
20°C	146 µm	1	1.5

Table 3. Aerosol specifications

Aerosol type	Initial aerosol diameter (µm)	Initial aerosol standard deviation	Aerosol mass injected (mg)
SiC	2	1.5	1800

3. SPRAY CHARACTERIZATION

Water spray is produced by a nozzle (TG_3.5) from Spraying System, with an internal diameter of 1 mm, which produces droplets of an almost uniform size. Spray characterization has been performed by the means of optical diagnostics in order to determine the initial droplets velocity, droplets size and spray angle. The spray angle is an important parameter because we have to check that droplets do not reach the vertical heated wall of the TOSQAN vessel, in order to prevent droplets vaporization. The spray angle was determined using the laser visualization technique as shown in Fig.2. An example of droplets size measurement performed by ILIDS technique is presented in Fig.3. ILIDS measurements were not performed close to the nozzle exit because of the high droplets density which causes multi-scattering phenomena and droplets overlapping. The mean vertical and radial velocities of droplets measured close to the nozzle exit by the PIV technique are presented in Fig.4 and Fig.5. In both velocity fields, the spray nozzle is located at a height (z) equal to 100 mm. The reference for the vertical velocity is negative for falling droplets. In Fig.4, the shear layer between the gas and the spray in the vertical velocity field resulting from the momentum exchange between the two phases of the flow can be observed. The radial velocity field shown in Fig.5 shows a usual pattern of spray expansion due to droplets inertia, with the radial velocity component close to zero in the center-part of the spray. Others droplets velocity measurements were performed in the field remote from the nozzle exit, in order to obtain a vertical profile of droplets velocities (Fig.7), and radial profiles of droplets velocities at different distances from the nozzle (Fig. 6). Droplet velocity measurements cannot be performed very close to the nozzle exit, which is the primary atomization zone with liquid ligaments. The initial droplets standardized velocity measured at 20 mm from the nozzle exit is therefore about 12 m.s^{-1}. A characteristic flat velocity profile can be observed at 50 mm from the nozzle exit. This kind of profile which delimits the spray area is typical of the near field of spray where the penetration of gas inclusions within the liquid core is not very efficient due to the high droplets density[8]. At the spray periphery a counter-flow loop shown by a positive velocity can be distinguished. On the other radial profiles, the spray development in relation to the distance from the nozzle exit can be observed, showing a decrease in droplets velocity resulting from momentum exchange with the gas. The gas entrainment induced by the spray droplets is underlined by the gas velocity field presented in the Fig. 8.

Gas entrainment is an important phenomena for the gas mixing inside the vessel and also for the aerosols removal process because the spray section is lower than the vessel section. Those points will be investigated during the further parts of this paper.
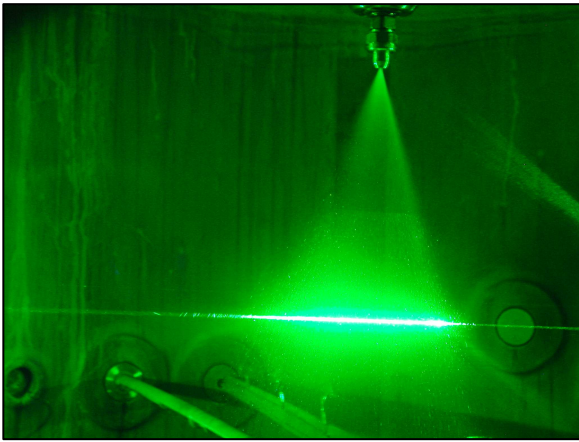
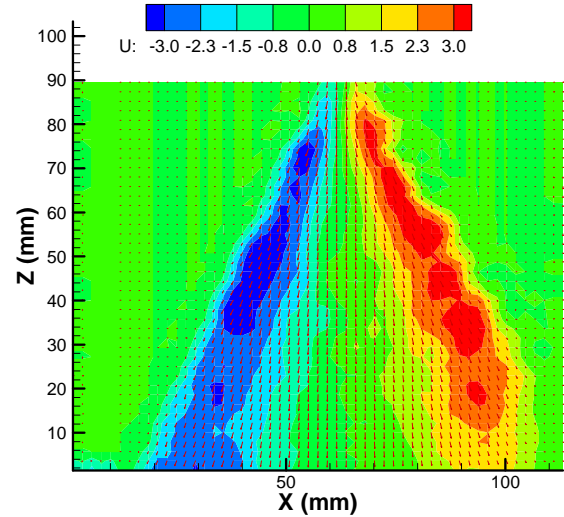Fig.2 Spray visualization in the TOSQAN vessel.

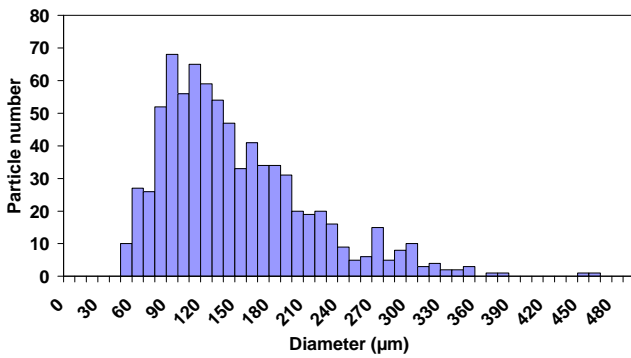Fig.5 Spray droplets radial velocity U (m.s^{-1}) field measured in the TOSQAN vessel.

Fig.3 Droplets size distribution (ILIDS measurements performed at 1 m from the nozzle exit) – Arithmetic mean diameter value equal to 146 µm.
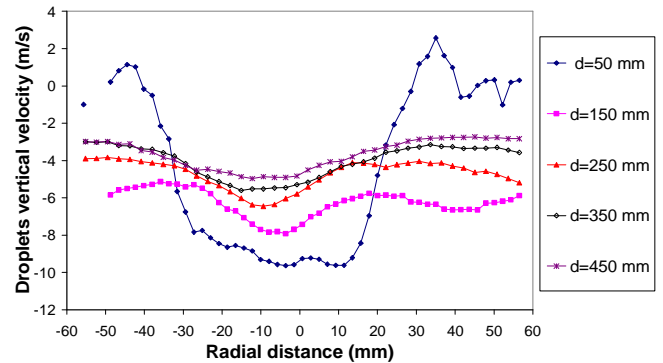

Fig. 6. Spray droplets vertical velocity measured on radial profiles in the TOSQAN vessel (extracted from PIV measurements).
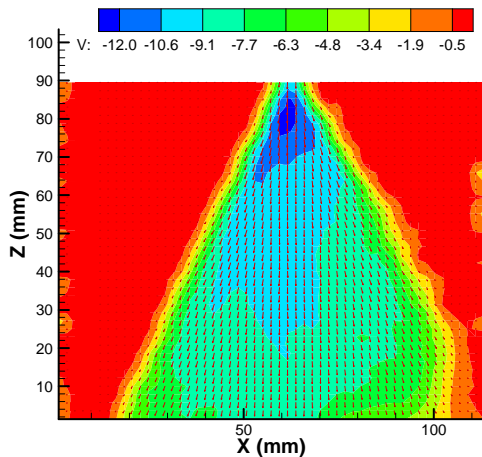

Fig.4 Spray droplets vertical velocity V (m/s) field measured in the TOSQAN vessel.
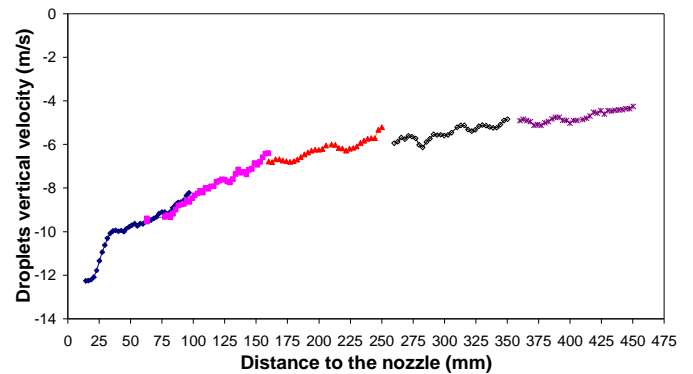

Fig.7 Spray droplets vertical velocity measured on vertical profile in the TOSQAN vessel (extracted from PIV measurements).
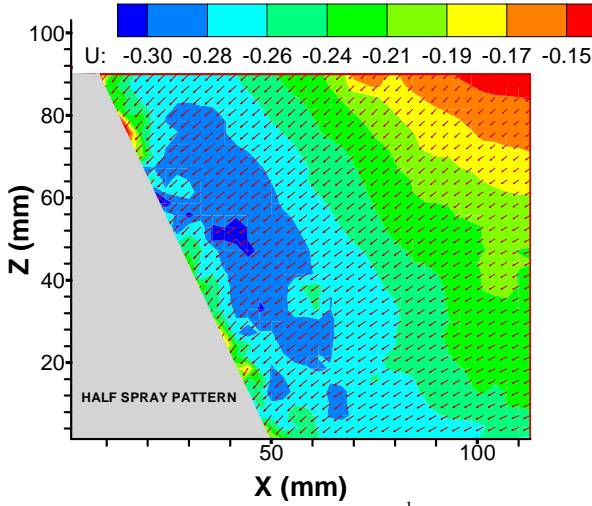
Fig. 8. Half gas radial velocity U (m.s^{-1}) field measured in the TOSQAN vessel.

4 ANALYSIS OF SPRAY INTERACTION WITH GAS MIXTURE

We made an overall analysis of the test conducted with the air and steam mixture. Time evolutions of vessel relative pressure and mean gas temperature are shown in Fig.9. Steam injection is started at the time reference t = - 500 s. The reference time t = 0 s corresponds to spray activation. The global Saturation Ratio SR(t), the steam saturated pressure $P_{saturation}$(t) and the gas mole number n_{gas_moles}(t) present in the vessel are computed in relation to time using Eq. (1), Eq. (2) and Eq. (3) for the test. Finally, the results are presented on the curve, such as the mean gas temperature (multiplied by 4 for scaling reasons), the global Saturation Ratio and the gas moles number (Fig.10).

$$SR(t) = \frac{P_{steam}(t)}{P_{saturation}(t)} \qquad (1)$$

The steam saturated pressure can be expressed with the following expression[9].

$$P_{saturation}(t) = \frac{10^5}{760} 10^A \qquad (2)$$

With $A = 16.37 - \dfrac{2818}{T_{gas\_mean}(t)} - 1,69 \log T_{gas\_mean}(t)$
$-5,75.10^{-3} \cdot T_{gas\_mean}(t) + 4,01.10^{-6} T^2_{gas\_mean}(t)$

$$n_{gas\_moles}(t) = \frac{P_{TOSQAN\_relative}(t).V_{TOSQAN}}{R.T_{gas\_mean}(t)} \qquad (3)$$

Where, $T_{gas\_mean}(t)$ is the mean gas temperature in the TOSQAN vessel, $P_{steam}(t)$ is the steam partial pressure and $P_{TOSQAN\_relative}(t)$ is the relative pressure in the vessel, in relation to time t.

The mean gas temperature is the spatial average of gas temperatures measured with thermocouples located along the vessel diameter at 6 different levels distributed along the TOSQAN height. Gas temperature fields measured at different times during the test are shown in Fig.11 and Fig.12.
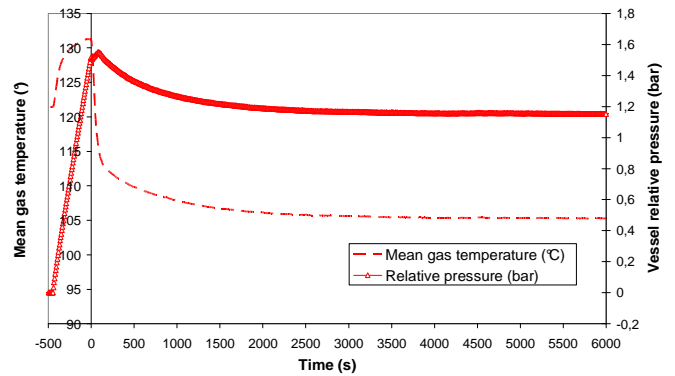

Fig.9 Time evolutions of vessel relative pressure and mean gas temperature during the tests (spray is activated at t = 0 s).
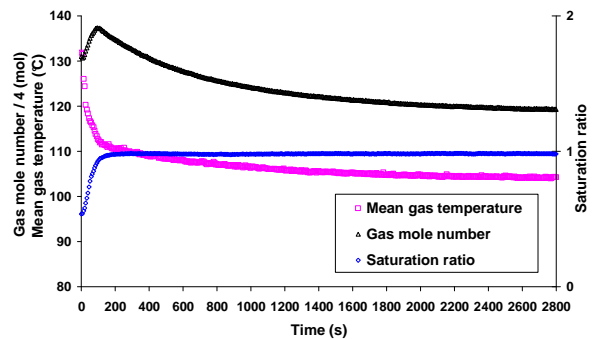

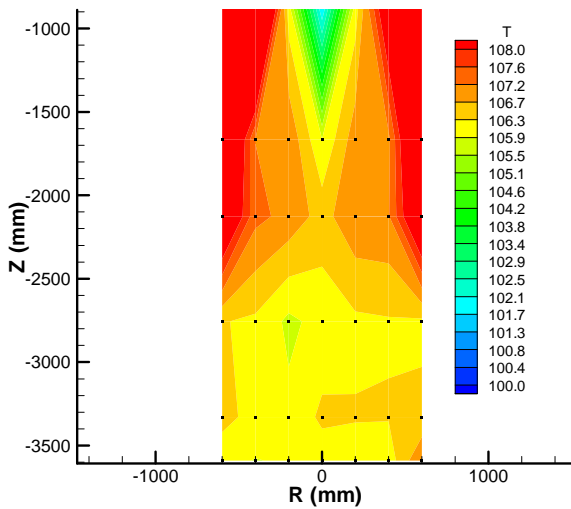Fig.10 Time evolutions of Saturation Ratio, gas mole number and mean gas temperature.

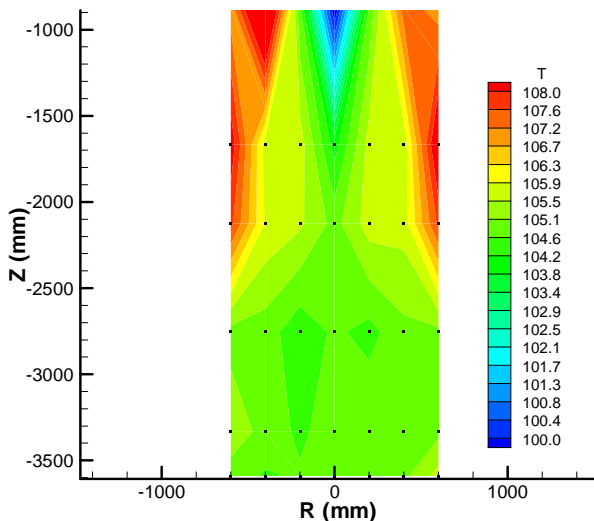Fig.11 Gas temperature (°C) field in the TOSQAN
vessel measured at t = 300 s.

Fig.12 Gas temperature (°C) field in the TOSQAN
vessel measured at t = 3000 s.

According to the results presented in the Fig.10, the test can be decomposed in different significant phases. At the beginning of spray activation (0 s < t < 100 s), a strong decrease of the vessel mean gas temperature, correlated with an increase in the saturation ratio, was observed. Spray activation is also followed by an initial overpressure generated by the increase of the gas mole number present in the vessel as shown in Fig.10. Nevertheless, as the vessel leak flow rate is negligible, the air mole number is constant in the vessel; consequently, the total mole number variation is equal to the evolution of the steam mole number in the containment. We can therefore conclude that during this time, spray droplets are vaporizing and therefore

produce a steam source. This first phase of droplets vaporization is due to a low initial saturation ratio and to an initial mass stratification, particularly in the bottom of the vessel. During this phase, the mean gas temperature is above of the heated walls temperature (120°C) leading to the activation of the heat exchanger that controls the wall temperature. But the effect on the decrease in mean gas temperature is slight compared to that produced by the spray activation. At the end of this phase (t = 100 s), the saturation ratio is practically at its equilibrium value equal to 1, meaning that the gas mixture is almost saturated by the steam. The second phase of the test is characterized by a strong decrease in the vessel pressure, gas mole number and mean gas temperature. During this phase (t > 100 s), steam condensation on water droplets is the dominant phenomenon. The gas mixture is cooled by convective heat transfer with the droplets initially injected at 20°C that induces steam condensation on droplets in order to keep a saturated mixture. The cooling effect of the spray is clearly shown in Fig.11 that also shows the non-uniformity of the gas field in the vessel.

The third phase of the test is characterized by a steady state with no significant changes in pressure, gas mole number, saturation ratio and mean gas temperature (t > 2500 s). The gas temperature field given in Fig.12 shows a homogeneous pattern except near the vertical heated walls and in the spray area. The decrease in the gas temperature scatter, compared to that observed for the first phase, is the consequence of the renewal of the gas, caused by the circulation loop resulting from the spray entrainment. During this phase, the energy provided to the droplets by the gas is compensated by that provided by the heated walls to the gas.

5 STUDY OF AEROSOL REMOVAL BY SPRAY
5.1 Time evolution of aerosol diameter during spray injection

In this section we focus on the aerosol behaviour during the spray injection. During the entire test, aerosol concentration and aerosol size present in the gas are measured in real time using optical granulometer[10]. From the time where the spray is activated, the aerosol mass collected by the spray droplets is also measured in real time. For this test, according to the spray angle, droplets don't impact the vertical walls of the vessel. So, we consider that the aerosol mass issued from the water drained along the vertical walls is negligible. For all the results presented on the following curves, the spray activation corresponds to the time t = 0 s. Time evolution of aerosol diameter is presented in Fig.13. In this figure is also presented the time evolution of aerosol number for different ranges of size. Spray activation induces a

strong decrease of the aerosol mean diameter according to the mechanical effects[11] and phoretic effects[12] involved in the removal of aerosol from the containment atmosphere by spray droplets. We can notice that the aerosol mean diameter decrease is more marked during the first two phases of the tests defined from Fig.10 in the previous section. Actually, for t < 2500 s, the aerosol removal process is more efficient for the largest aerosols which are collected by droplets, mainly due to mechanical effects. Phoretic effects such as diffusiophoresis are relative to steam concentration gradient around the droplets. Diffusiophoresis will be involved in the removal process during the phase of the test where heat and mass transfers between droplets and gas, such as steam condensation on droplets, are strong.

So, at t = 2500 s, according to sedimentation, aerosol collection by droplets due to mechanical effects and subsidiary, due to diffusiophoresis, aerosols which diameter is larger than 2 µm are not present in the gas anymore.
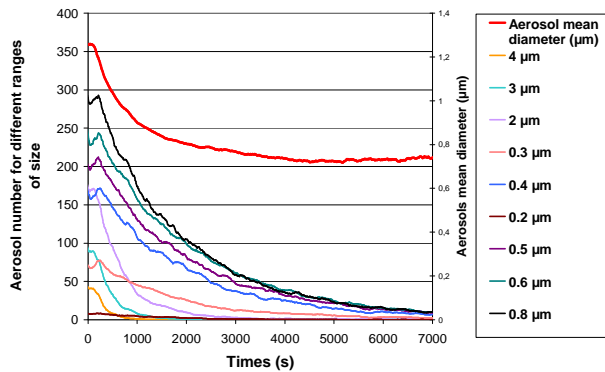

Fig.13 Time evolution of the aerosol mean diameter and aerosol number by range of size.

In order to analyse the global spray collection efficiency as a function of aerosol size distribution, aerosol histograms size obtained at different times, before and during spraying, are presented in Fig.14. The global spray efficiency for aerosol removal, which is the ratio between the difference of the particles number present in the gas before spraying and at t = 4000 s, with the particles number present before spraying, is also plotted in Fig.14. The global spray collection efficiency tends towards 1 for aerosol which size is larger than 1 µm. As we can see, the global spray efficiency seems to have a minimum for aerosol size around 0.5 µm. This result corresponds to the fact that, for these ranges of aerosol and droplet size, mechanical effects have a poor efficiency and thermophoresis effects become negligible[13].
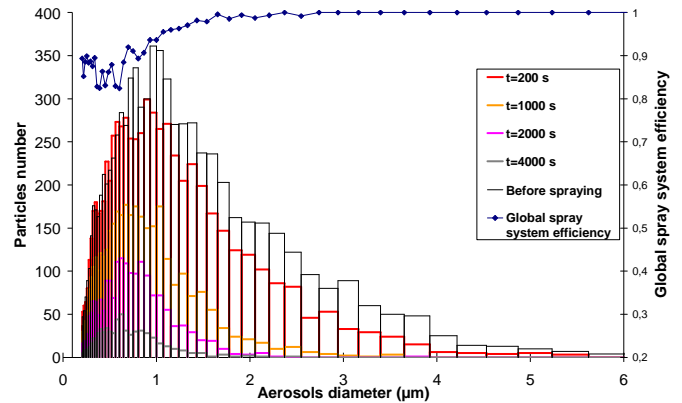

Fig.14 Aerosol size distributions at different time.

5.2 Aerosol removal rate and droplet collection efficiency

In this part, we investigate the aerosol removal rate (λ_s) and the single droplet collection efficiency (E) during the test. The single droplet efficiency is defined as the ratio between the aerosol mass collected by a droplet and the aerosol mass present in the swept out volume. We need to measure the global aerosol mass collected by spray droplets at each time step. As aerosol concentration is expected to be different in the spray region and in the dry region, during spray injection, the WELAS granulometer measurement which is a local measurement, can not be used to determine the total aerosol mass present in the gas of the vessel. On the other hand, before spray activation, the aerosol mass concentration present in the gas ($C_{aerosol}(0)$) can be determined using WELAS granulometer measurement because the aerosol mass concentration is homogeneous in the gas of the vessel due to mixing induced by steam injection. It is why one can extrapolate the total aerosol mass in the vessel ($M_{aerosol\_gas}(0)$) (Eq. 4) from the local measurement performed with the WELAS granulometer. During spray activation, the global aerosol mass collected by spray droplet at each time step ($M_{aerosol\_collected}(t)$) is measured with the turbidimeter. The total aerosol mass present in the gas at the instant t $\left(M_{aerosol\_gas}(t)\right)$ (Eq. 5) is obtained experimentally with the difference between the initial aerosol mass present at t = 0 s (Eq. 4) and the aerosol mass collected by the spray at the instant t $\left(M_{aerosol\_collected}(t)\right)$.

$$M_{aerosol\_gas}(0) = C_{aerosol}(0).V_{TOSQAN\_vessel} \qquad (4)$$

$$M_{aerosol\_gas}(t) = M_{aerosol\_gas}(0) - M_{aerosol\_collected}(t)$$

$$(5)$$

On the other hand, the total aerosol mass present in the gas at the instant t can also be defined in using the aerosol removal rate λ_s by the Eq. 6.

$$M_{aerosol\_gas}(t) = C_{aerosol}(0).\exp-(\lambda_s t).V_{TOSQAN\_vessel}$$

(6)

The evolution of the total aerosol mass present in the gas of the vessel (Eq. 5) is presented in Fig.15.
At spray activation (t = 0 s), the initial total aerosol mass in suspension in the vessel equals 1238 mg which is less than the aerosol mass injected in the vessel before spray activation (m=1500 mg). This difference may be related to aerosol deposition on vertical walls induced by the development of a wall turbulent boundary layer.
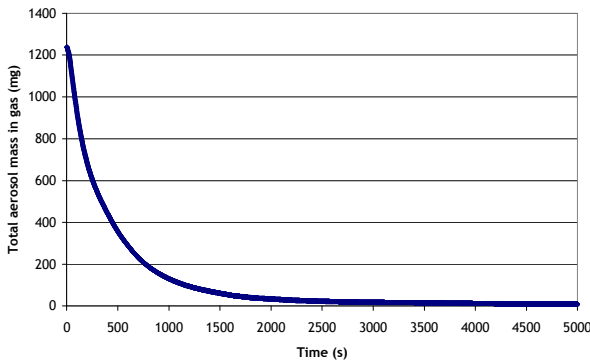

Fig.15. Time evolution of the aerosol mass in the gas of the vessel (mg)

Use of the Postma[14] equation (Eq. 7) allows computing the single droplet collection efficiency (E) from the aerosol removal rate (λ_s). The Postma relation links the droplet collection efficiency to spray and vessel parameters such as droplet size ($D_{droplet}$), droplet falling height (h), vessel volume (V_{TOSQAN_vessel}) and water spray mass flow rate ($Q_{spray\_volumic}$).

$$\lambda_s = \frac{3}{2} \frac{Q_{spray\_volumic}.h}{D_{droplet}.V_{TOSQAN\_vessel}}.E \quad (7)$$

With:
h = 4 m
$$Q_{spray\_volumic} = 30.10^{-6} m^3 s^{-1}$$
V_{TOSQAN_vessel} = 7 m³
$D_{droplet}$ = 146 µm

Some assumptions are necessary to use the Postma relation such as the whole vessel volume is covered by monodispersed spray droplets, and the aerosol mass concentration is homogeneous in the vessel. For TOSQAN test, according to the spray angle (57°), the sprinkled volume corresponds to 75% of the vessel

volume. The droplet size distribution is not strictly monodispersed, but from the results presented in the Fig.3, we can see that the droplet size distribution is relatively centred. The aerosol mass concentration is expected to be homogeneous inside the spray region. So, the curve showing the time evolution of the aerosol mass in gas (Fig.15) is fitted from time equal to 200 s to time equal to 1500 s to determine the aerosol removal rate (Fig.16). At the time of the spray activation, a transient phase of water draining occurs in the sump bottom and the online turbidimeter measurement can not be directly related to the aerosol mass collected by spray droplets. The duration of the draining phase was determined to be 200 s, and measurements taken during this time period are discarded. At the same time, measurements obtained for t > 1500 s are not considered, due to the increase of the online turbidimeter accuracy observed for lower aerosol mass concentration present in draining water.
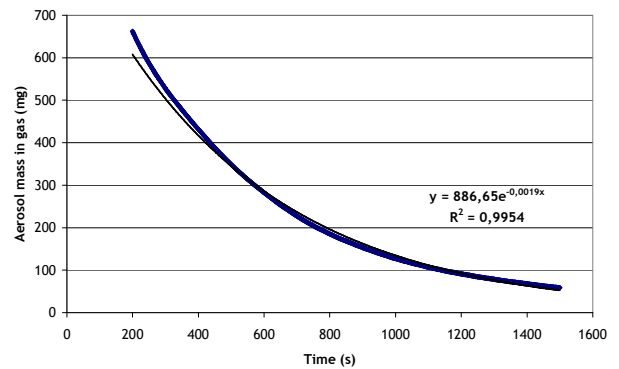

Fig.16. Time evolution of the total aerosol mass present in the gas inside the vessel from t = 200 s to t = 1500 s. Determination of aerosol removal rate from the curve fitting

According to the result presented on the Fig.16, the aerosol removal rate is equal to 0.0019 during the period 200 s to 1500 s. In this condition, the droplet collection efficiency computed with the relation (7) is equal to 0.0108 which is in good agreement between Powers's results for droplet size of 200 µm[15] and with Ducret's results[16] for monodisperse droplet size of 280 µm. Let's point out the fact that Ducret's results were obtained during steady state thermal-hydraulic conditions and aerosol mass concentration in suspension in the CARAIDAS vessel, and the single droplet collection efficiency is constant during the test, as opposed to the TOSQAN vessel where the aerosol population changes all along the test. Another approach was to determine the elementary droplet collection efficiency versus time for each aerosol range of size to determine the droplet collection efficiency. In order to calculate the elementary droplet collection efficiency,

we suppose that the aerosol mass loss in the gas is only due to droplet collection phenomena and transfers from the gas surrounding to spray area. This transfer is due to the gas entrainment induced by the spray droplets (Fig. 8). The droplets are supposed to be also monodispersed. The droplets collection efficiency is then computed in using the local loss of aerosol mass in the gas between two time steps, measured with the WELAS granulomter. Results which are presented in the Fig. 17, show that the minimum of efficiency is obtained for aerosol size slightly lower than 1 µm. The minimum corresponds to the fact that the collection mechanisms based on Brownian diffusion and thermophoresis become negligible and droplets collection mechanisms based on impaction and interception are not yet important[17] .
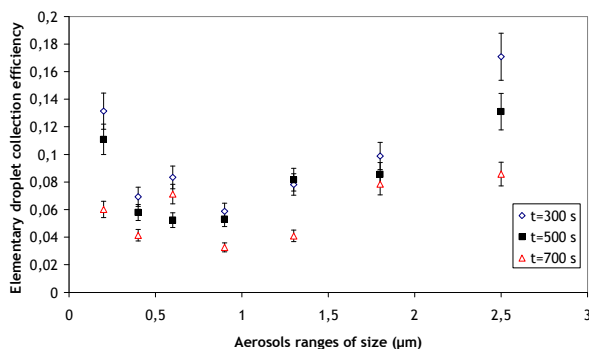

Fig. 17. Elementary droplet collection efficiency versus aerosols ranges of size, at different times.

6. COMPARISON BETWEEN EXPERIMENTAL AND NUMERICAL RESULTS

The French-German integral code ASTEC (Accident Source Term Evaluation Code[18]) is developed commonly by IRSN and GRS with the aim to get a fast-running code for the simulation of the complete sequences of severe accidents in LWR (Light Water Reactors), from the initiating event up to the possible fission products release to the environment. The code can be applied to accidental sequence studies, probabilistic safety assessments, investigations on accident management procedures and support to tests. ASTEC is the European software of reference in the network of excellence SARNET (Severe Accident Research NETwork). For this study, the interesting module for the aerosol collection by droplet of the spray is the CPA module (Containment Part of ASTEC: Thermohydraulics & Aerosol behaviour in Containment[19]). The TOSQAN vessel mesh is composed of 2 coaxial cylinders. The compartment located at the centre of the vessel defines the spray region. The coaxial cylinder which defines the gas

region is divided in two parts, the upper and the lower region. This mesh organization allows representing aerosol transfer from the gas region to the spray region, due to spray entrainment. The aerosol mass collected by spray droplet and also the total aerosol mass deposited on the walls is calculated with ASTEC code. For ASTEC calculation, the vessel initially pressurized with steam is seeded with aerosol from t = -300 s to t = -250 s (Fig. 19). From t = - 300 s to spray activation at t = 0 s, ASTEC calculation shows the evolution of the aerosol mass which is deposited on the vertical walls and on the bottom of the vessel. ASTEC results show that about more than 10 % of the initial aerosol mass injected in the vessel is deposited on vessel wall. This deposited aerosol mass will not be drained to the sump during spraying. From the time where the spray is activated, the deposited aerosol mass becomes negligible comparatively to spray droplet wash out processes because of the higher transport coefficient due to the falling droplet[20]. The comparison between ASTEC calculation and experimental results are presented in the Fig.18. The comparison is based on the aerosol mass collected by the spray in the central compartment including the aerosol mass which has been settled on the sump bottom. Results presented in Fig show a good agreement between experimental and numerical approaches especially concerning the dynamic of aerosol mass evolution from the beginning of the test to t = 1500 s which corresponds to the phase where the largest aerosol have been collected by spray droplet. This results show that mechanisms of aerosol collection by droplet and of aerosol transfer to spray region are well described in ASTEC code. We can notice that there is difference between the experimental and numerical value of the total aerosol mass collected by spray droplet. But this difference (almost 7 %) is the same order of magnitude as the turbidimeter experimental uncertainty (see Table 1). Another explanation may be linked to the calculation of the aerosol mass deposited on wall by the ASTEC code. We can conclude that the ASTEC code is efficient to predict quantitatively the aerosol collection mechanisms.
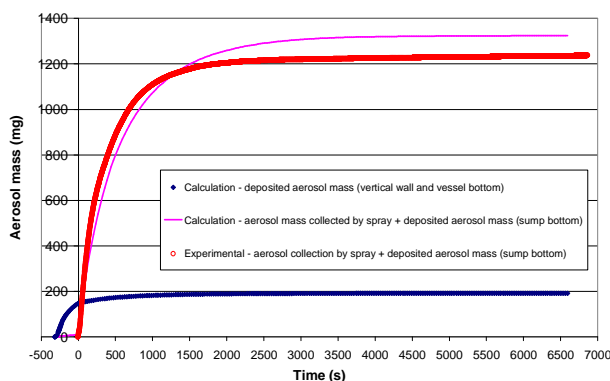
Fig. 18. Comparison between experimental and numerical results: aerosol mass evolution in the vessel

7 CONCLUSION

Spray tests with aerosol were conducted in the TOSQAN large facility devoted to thermal hydraulic containment studies. Spray tests realized in hot conditions allow us to study the interaction between spray droplets and gaseous mixtures such as air and steam, seeded with aerosol simulating fission products. Advanced instrumentation was developed, implemented and qualified on the TOSQAN facility in order to characterize all the magnitudes required for analysing the effect of spray injection on containment thermal hydraulic conditions and also, the local heat and mass transfers between spray droplets and gas. Detailed measurements such as the droplet velocity, droplet size, aerosol size and concentration, gas volume concentrations, gas temperature and pressure were then performed during the tests. First, an overall analysis was conducted to explain the different phases of the spray test, such as the initial steam overpressure induced by droplets vaporization followed by a strong vessel depressurization due to steam condensation on droplets and convective heat transfer between droplets and gas. The last phase identified is a steady state for which the energy provided to the droplets by the gas is compensated by that provided by the heated walls to the gas. Aerosol removal by spray droplets was studied in order to quantify the global spray collection efficiency and the single droplet collection efficiency. Results show that aerosols which size is above than 2 µm are rapidly washed out by the spray. Spray efficiency is less good for smaller aerosol for which droplets collection by mechanical effects has a poor efficiency, according to droplet size. The single droplet collection efficiency was computed with both approaches, the first one based on a global measurement of the aerosol mass collected by the droplets, and the second one based on the local evolution of the aerosol mass present in the gas at each time step of the test. The results obtained for thermal hydraulic conditions representative of severe accident in the TOSQAN vessel show a good agreement with literature studies. The comparison of numerical ASTEC code results with experimental results shows globally a good agreement for this test. In the next future, spray tests with aerosol will be performed to analyse the effect of spray and aerosol parameters on aerosol removal processes[21].

REFERENCES

(1) Fermandjian, J., Comportement des aérosols dans l'enceinte de Confinement, SFRP - Meeting on mitigation and confinement of radioactive products in water cooled reactors, Saclay, 1984.

(2) Porcheron E., Lemaitre P., Nuboer A., Rochas V. and Vendel J. Experimental investigation in the TOSQAN facility of heat and mass transfers in a spray for containment application, Nuclear Engineering and Design, Volume 237, Issues 15-17, September 2007, Pages 1862-1871, 2007.

(3) Auban, O., Malet, J., Brun, P., Brinster, J., Quillico, J., Studer, E., Implementation of gas concentration measurements systems using mass spectrometry in containment thermal hydraulic test facilities: Different approaches for calibration and measurement with steam/air/helium mixtures, Proceedings of the NURETH-10, Seoul, 2003.

(4) Mölter, L. and Keßler, P., Partikelgrößen- und partikelanzahlbestimmung in der außenluft mit einem neuen optischen aerosolpektrometer, Gefahrstoffe Reinhaltung der Luft, Vol. 64, (10), pp. 439-447, 2004.

(5) Bachalo, W.D., Houser, M.J., 1984. Phase/Doppler spray analyzer for simultaneous measurements of drop size and velocity distribution, Optical Engineering, Vol. 23, No. 5, pp. 583-590.

(6) Lemaitre, P., Porcheron, E., Nuboer, A., Grehan, G.,. Interferometric laser imaging development in order to measure droplet size in hostile environment, Proceedings of the ICLASS, Kyoto, 2006.

(7) Porcheron E., Thause L., Malet J., Cornet P., Brun P., Vendel J., Simultaneous application of spontaneous Raman scattering and LDV, PIV for steam-air flow characterization, Proceedings of the 10ᵗʰ Int. Symposium on Flow Visualization, Kyoto, 2002.

(8) Porcheron, E., Carreau, J.L., Prevost, L., Roger, F., 2002. Effect of gas density injection on assisted cryogenic liquid jet atomization, Atomization & Sprays, pp. 209-227, Vol. 12.

(9) Haar, L., Gallager, J.S. and Kell, G.S., NBS/NRC Steam Tables, Hemisphere Publishing Corp., New York, 1984.

(10)Marchand, D., Porcheron, E., Lemaitre, P. and Grehan, G., Characterization of the washout of aerosol by spraying water for thermal hydraulic conditions representative of a severe accident in a nuclear reactor containment, ICLASS, Kyoto, 2006.

(11)Rimberg, D. and Peng , Y., Aerosol collection by falling droplets, Air pollution Control and Design Handbook, New York, 1977.

(12)Waldmann, L. and Schmitt, K. H., Thermophoresis and diffusiophoresis of aerosol, C.N. Davies, 1966.

(13)Murata, K., K., Williams, D., C., Tills, J., Griffith, R., O., Gido, R., G., Tadios, E., L., Davis, F., J., Martinez, G. and Washington, K., E., Code Manual for CONTAIN 2.0: A computer Code for Nuclear Reactor Containment Analysis, NUREG/CR-6533, SAND97-1735, Sandia National Laboratories, Albuquerque, New Mexico.

(14)Postma, A. K., Sherry, R. R. and Tam, P. S. (1978) Technological bases for models of spray washout of airborne contaminants in containment vessels. NUREG/CR-0009, Nuclear Regulatory Commission, Office of Nuclear Reactor Regulation, Division of Site Safety and Environmental Analysis, Accident Analysis Branch ; for sale by the National Technical Information Service.

(15)Powers, D. A. and Burson, S. B., A Simplified Model Of Aerosol Removal by Containment Sprays, NUREG/CR-5966, SAND92-2689, 1993.

(16)Ducret, D., Roblot, D. and Vendel, J., Etude analytique du comportement des gouttes et du rabattement des produits de fission par l'aspersion : résultats expérimentaux et modèles, OECD Specialist Meeting On Nuclear Aerosol In Reactor Safety, Cologne, 1998.

(17)Murata, K. K., Williams, D. C., Tills, J., Griffith, R. O., Gido, R. G., Tadios, E. L., Davis, F. J., Martinez, G. M. et Washington, K. E, Code Manual for CONTAIN 2.0 : A Computer Code for Nuclear Reactor Containment Analysis. NUREG/CR-6533, SAND97-1735, Sandia National Laboratories, Albuquerque, NM, 1997.

18. Allelein, H. J., Neu K. and Van Dorsselaere J.P., European Validation of the Integral Code ASTEC (EVITA): First experience in validation and plant sequence calculations, *Nuclear Engineering and Design*, (**235**), pp.285-308, 2005.

19. Plumecocq, W., Layly, V. D. and Bentaib, A., Modelling of the containment mitigation mesures in the ASTEC code, Focusing on spray hydrogen recombiners, NURETH-11, 2005.

(20)Postma A. K., Coleman L. F., Effect of continuous spray operation on the removal of aerosol and gases in the containment systems experiment, BNWL-1485, 1970.

(21)Marchand, D., Experimental and numerical approaches for aerosol removal for containment spray application, Thesis of University of Rouen, work in progress